



**HAL**  
open science

## First-order numerical analysis of linear thin layers

Frédéric Lebon, Sylvie Ronel-Idrissi

► **To cite this version:**

Frédéric Lebon, Sylvie Ronel-Idrissi. First-order numerical analysis of linear thin layers. *Journal of Applied Mechanics*, 2007, 74 (4), pp.824-828. 10.1115/1.2424716 . hal-00106899

**HAL Id: hal-00106899**

**<https://hal.science/hal-00106899>**

Submitted on 19 Jun 2018

**HAL** is a multi-disciplinary open access archive for the deposit and dissemination of scientific research documents, whether they are published or not. The documents may come from teaching and research institutions in France or abroad, or from public or private research centers.

L'archive ouverte pluridisciplinaire **HAL**, est destinée au dépôt et à la diffusion de documents scientifiques de niveau recherche, publiés ou non, émanant des établissements d'enseignement et de recherche français ou étrangers, des laboratoires publics ou privés.

# First-Order Numerical Analysis of Linear Thin Layers

F. Lebon<sup>1</sup>

Laboratoire de Mécanique et d'Acoustique,  
Université Aix-Marseille 1,  
31 Chemin Joseph-Aiguier,  
13402 Marseille Cedex 20, France  
e-mail: lebon@lma.cnrs-mrs.fr

S. Ronel

Laboratoire de Biomécanique et de Modélisation  
Humaine,  
Université Lyon 1,  
IUT B,  
17 rue de France,  
69100 Villeurbanne, France  
e-mail: sylvie.ronel@iutb.univ-lyon1.fr

*This paper deals with the first-order numerical analysis of thin layers. Theoretical results are recalled and compared with numerical data obtained on two classical examples. The effects of concentrated forces are discussed. [DOI: 10.1115/1.2424716]*

## 1 Introduction

The aim of this study was to perform a first-order asymptotic and numerical analysis on linear thin layers. The rigidity of the thin layers is assumed here *not to depend on its thickness*. During the last few decades several authors have developed asymptotic theories applied to thin layers (see Ref. [1]). These problems have mostly been studied at order zero, and only a few authors have performed **first-order** studies [2]. We assume that only the geometrical parameter of the layer (the thickness) tends towards zero, and, analyze the limit problem using matched asymptotic expansions [3]. In this limit problem, the layer vanishes geometrically and is replaced by an interface. The aim of this study is to check *quantitatively* the validity of the theoretical approach. This point is a crucial one for mechanical engineers because in practice, the thickness of the thin layer is generally very small.

The paper is organized as follows: in Sec. 2, the mechanical problem and the theoretical results are presented. Section 3 deals with two numerical examples. In Sec. 4, we analyze the influence of the concentrated forces obtained in the theoretical limit problem. In Sec. 5, we draw some conclusions and discuss the perspectives.

## 2 The Mechanical Problem and Theoretical Results

Let us consider two elastic bodies which are perfectly bonded with a third one which is very thin. For sake of simplicity, we work only in two dimensions. The structure is denoted  $\Omega$  with boundary  $\partial\Omega$  and is referred to the local frame  $(O, x_1, x_2)$ . A surface load is applied to the part of the structure  $\Gamma_1$ . The structure is embedded in part  $\Gamma_0$ . We take  $\Omega_\varepsilon$  to denote the part of  $\Omega$  such that  $|x_2| > \varepsilon/2$  (the adherent) and  $B_\varepsilon$  to denote the complementarity part  $\Omega/\Omega_\varepsilon$  (the adhesive). Segment  $S$  is the intersection between  $\Omega$  and the line  $\{x_2=0\}$ . We adopt the small perturbations hypoth-

esis and the adhesion between  $\Omega_\varepsilon$  and  $B_\varepsilon$  is assumed to be perfect. Note that  $S$  is the surface to which the adhesive tends geometrically. The material composing is assumed to be elastic. We take  $\lambda$  and  $\mu$  to denote the Lamé coefficients of the adhesive. Contrary to more classical studies, the order of magnitude of the stiffness is assumed to be the same in the adherent and in the adhesive (see Fig. 1).

**2.1 Presentation of the Problem.** In what follows, a jump across  $S$  is denoted by  $[\cdot]$  and a jump across the interface  $S_\varepsilon$  between  $\Omega_\varepsilon$  and  $B_\varepsilon$  is denoted by  $[\cdot]_\varepsilon$ . The equations of the problem are written as follows ( $\boldsymbol{\sigma}$  denotes the stress tensor and  $\mathbf{u}$  the displacement vector):

$$\begin{aligned} \operatorname{div} \boldsymbol{\sigma} &= 0 \text{ in } \Omega \\ \boldsymbol{\sigma} \mathbf{n} &= \mathbf{F} \text{ on } \Gamma_1 \\ \mathbf{u} &= 0 \text{ on } \Gamma_0 \\ [\mathbf{u}]_\varepsilon &= 0 \text{ on } S_\varepsilon \\ [\boldsymbol{\sigma} \mathbf{n}]_\varepsilon &= 0 \text{ on } S_\varepsilon \end{aligned} \quad (1)$$

The constitutive equations are written as follows ( $\mathbf{e} = \mathbf{e}(\mathbf{u})$  denotes the strain tensor)

$$\begin{aligned} \boldsymbol{\sigma} &= \mathbf{A} \mathbf{e}(\mathbf{u}) \text{ in } \Omega_\varepsilon \\ \boldsymbol{\sigma} &= \lambda \operatorname{tr}(\mathbf{e}(\mathbf{u})) \mathbf{I} + 2\mu \mathbf{e}(\mathbf{u}) \text{ in } B_\varepsilon \end{aligned} \quad (2)$$

In the previous equation,  $\mathbf{A}$  denotes a given elasticity tensor.

**2.2 Matched Asymptotic Expansions.** We assume that the solution of the above problem can be expanded into power series of  $\varepsilon$ . Using the matched asymptotic expansions method [4], we introduce internal (Eq. (4)) and external (Eq. (3)) expansions of the displacement vector  $\mathbf{u}^\varepsilon$  and the stress tensor  $\boldsymbol{\sigma}^\varepsilon$  which are valid sufficiently far from the edges. The two expansions are assumed to be coincident in a set of intermediate points (Eq. (5)). We write

$$\mathbf{u}^\varepsilon(x_1, x_2) = \sum_{m=0}^{\infty} \varepsilon^m \mathbf{u}^m(x_1, x_2), \quad \boldsymbol{\sigma}^\varepsilon(x_1, x_2) = \sum_{m=0}^{\infty} \varepsilon^m \boldsymbol{\sigma}^m(x_1, x_2) \quad (3)$$

$$\mathbf{u}^\varepsilon(x_1, x_2) = \sum_{m=0}^{\infty} \varepsilon^m \mathbf{v}^m\left(x_1, \frac{x_2}{\varepsilon}\right), \quad \boldsymbol{\sigma}^\varepsilon(x_1, x_2) = \sum_{m=0}^{\infty} \varepsilon^m \boldsymbol{\tau}^m\left(x_1, \frac{x_2}{\varepsilon}\right) \quad (4)$$

$$\mathbf{v}^0(x_1, \pm \infty) = \mathbf{u}^0(x_1, 0^\pm)$$

$$\boldsymbol{\tau}^0(x_1, \pm \infty) = \boldsymbol{\sigma}^0(x_1, 0^\pm)$$

$$\mathbf{v}^1(x_1, \pm \infty) = \mathbf{u}^1(x_1, 0^\pm) + \lim_{y \rightarrow \pm\infty} y \frac{\partial \mathbf{u}^0}{\partial x_2}(x_1, 0^\pm) \quad (5)$$

$$\boldsymbol{\tau}^1(x_1, \pm \infty) = \boldsymbol{\sigma}^1(x_1, 0^\pm) + \lim_{y \rightarrow \pm\infty} y \frac{\partial \boldsymbol{\sigma}^0}{\partial x_2}(x_1, 0^\pm)$$

Let  $y_2 = x_2/\varepsilon$ .

Introducing these expansions into Eqs. (1) and (2), we obtain

$$\tau_{ij}^n = \lambda e_{kk}^n \delta_{ij} + 2\mu e_{ij}^n, \quad n = 0, 1$$

$$\frac{\partial v_j^0}{\partial y_2} = 0, \quad j = 1, 2$$

$$e_{11}^0 = \frac{\partial v_1^0}{\partial x_1}$$

<sup>1</sup>Corresponding author.

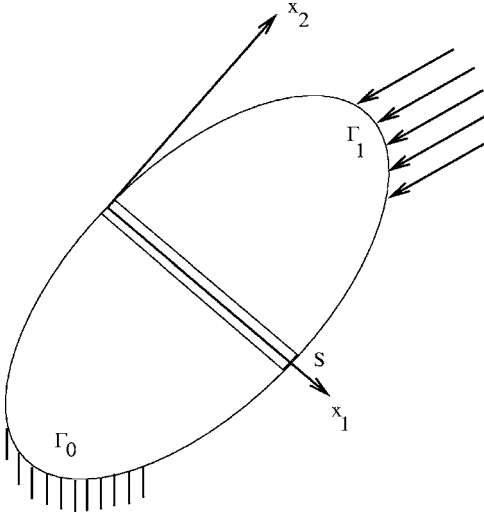


Fig. 1 The mechanical problem

$$\begin{aligned}
 e_{22}^0 &= \frac{\partial v_2^1}{\partial y_2} \\
 e_{12}^0 &= \frac{1}{2} \left( \frac{\partial v_2^0}{\partial x_1} + \frac{\partial v_1^1}{\partial y_2} \right) \\
 \frac{\partial^0}{\partial y_2} &= 0 \\
 \frac{\partial^0}{\partial x_1} + \frac{\partial^1}{\partial y_2} &= 0
 \end{aligned} \tag{6}$$

**2.3 Asymptotic Results.** By integration, Eqs. (5) and (6) (ii) mean that  $[u_i^0]=0, i=1,2$ . Likewise, Eqs. (5) and (6) (vi) mean that  $[\sigma_{i2}^0]=0, i=1,2$ . In conclusion, we have the following order zero system

$$[u_1^0](x_1) = 0 \tag{7a}$$

$$[u_2^0](x_1) = 0 \tag{7b}$$

$$[\sigma_{22}^0](x_1) = 0 \tag{7c}$$

$$[\sigma_{12}^0](x_1) = 0 \tag{7d}$$

In the same way, by integration, Eqs. (5) and (6) (i) with  $n=0$  and (6) (iii-v) mean that the jump in the displacements  $[u_i^1], i=1,2$  is not equal to zero and depends on  $\sigma_{i2}^0$  and  $\partial u_i^0/\partial x_1$ . The corresponding results are given in Eq. (8).

The jump in the stresses is obtained using Eqs. (5) and (6) (vii), and (6) (i) (by derivation). In conclusion, we have the following order one system

$$[u_1^1](x_1) = \frac{\sigma_{12}^0}{\mu} - \frac{\partial u_2^0}{\partial x_1} \tag{8a}$$

$$[u_2^1](x_1) = \frac{\sigma_{22}^0}{\lambda + 2\mu} - \frac{\lambda}{\lambda + 2\mu} \frac{\partial u_1^0}{\partial x_1} \tag{8b}$$

$$[\sigma_{22}^1](x_1) = -\frac{\partial \sigma_{12}^0}{\partial x_1} \tag{8c}$$

$$[\sigma_{12}^1](x_1) = -\frac{4\mu(\lambda + \mu)}{\lambda + 2\mu} \frac{\partial^2 u_1^0}{\partial x_1^2} - \frac{\lambda}{\lambda + 2\mu} \frac{\partial \sigma_{22}^0}{\partial x_1} \tag{8d}$$

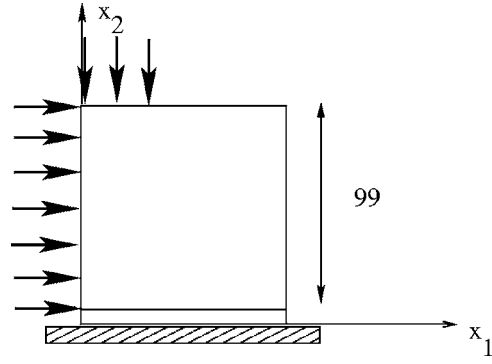


Fig. 2 First example: square bar bonded with a rigid body (dimensions in mm)

Note that the model obtained is **nonlocal**.

### 3 Numerical Tests

The aim of this section is to check quantitatively the validity of the theory. It is crucial to obtain values of the thickness for which it is possible to substitute the real problem by the limit one. The computations were performed using the ANSYS (Multiphysics solver, Plan82 element, plane stress) software program [5]. The discretization of the thin layer is done by two or four elements in the thickness and 200 elements in the width. This numerical section contains two parts, corresponding to two examples. In the first part, we observe the jumps in the displacements  $[u_1]$  and  $[u_2]$  and the jumps in the stress vector  $[\sigma_{22}]$  and  $[\sigma_{12}]$  along the interface zone (based on Eq. (7)). In the second one, we check the validity of Eq. (8).

#### 3.1 First Numerical Example

**3.1.1 Geometry of the Problem.** In this section, we describe numerical tests performed on a long square bar bonded with a rigid obstacle (Fig. 2). The width of the bar was equal to 99 mm and the thickness of the thin layer was equal to 1 mm. A horizontal load was applied to the whole left part of the structure and a vertical one was applied to only the upper left nodes of the square bar. The mechanical data are given in Table 1.

##### 3.1.2 Numerical Synthesis

**3.1.2.1 Jump in the displacements at order 0 (Eqs. (7a) and (7b)).** The first step in the numerical test consists of checking that the values of the jump in the displacements at order zero tend toward zero. In this example, the jump in the displacements is equal to the displacement of the upper nodes of the thin layer. It is confirmed that the displacement is small (see Figs. 4(a) and 4(b)). The values of the displacements tend toward zero: these values are in the  $[2 \cdot 10^{-4}, 5 \cdot 10^{-4}]$  mm range with  $u_1$  and in the

Table 1 Mechanical data

Example	1	2
thickness (mm)	1	1
Substrate: Young's modulus (GPa)	200	200
Substrate: Poisson ratio	0.3	0.3
Thin layer: Young's modulus (GPa)	160	160
Thin layer: Poisson ratio	0.3	0.3
Total $x_1$ force (N)	1800	1800
	(18 nodes)	(18 nodes)
Total $x_2$ force (N)	-1200	-1000
	(60 nodes)	(50 nodes)
Finite element	8-node	8-node
	quadrangle	quadrangle

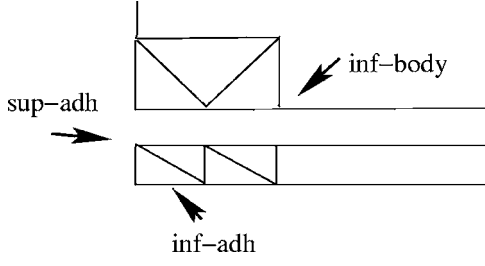


Fig. 3 First example: three lines of nodes

$[-3 \cdot 10^{-4}, 3 \cdot 10^{-4}]$  mm range with  $u_2$ . These values are approximately 100 times smaller than those in the adherent. It is noticed that in this modeling, contrary to other theories for which the rigidity of the adhesive is small, the jump in the displacements tends toward zero.

3.1.2.2 *Jump in the stress vector at order 0 (Eqs. (7c) and (7d)).* In the case of the stress vector, we computed three sets of values (Fig. 3): the lower and the upper nodes of the layer and the lower nodes of the body (Figs. 4(c) and 4(d)). The three curves (denoted inf-adh, sup-adh, and inf-body in Fig. 4) are very similar, the jump tends towards zero, and it is possible to choose any of these three values for the following computations. In particular, the computation of the gradient can be done indifferently on one of the three surfaces.

3.1.2.3 *Jump in the displacements at order 1 (Eqs. (8a) and (8b)).* In this case, the thin layer is bonded directly with a rigid body and some of the terms in Eqs. (8a) and (8b) can be simplified. In particular, the jump in the displacement at order zero is equal to zero as are the displacement and its  $x_1$  derivatives. Since the lower nodes are clamped, the jump in the displacements at order one is computed as the displacements of the upper nodes in the thin layer divided by  $\varepsilon$ . In Eq. (8a) the jump in the displacement of  $u_1$  at order one is approximately  $\sigma_{12}$  at order zero divided by  $\mu$  (Fig. 5(a)). In Eq. (8b) the jump in the displacements of  $u_2$  at order one is approximately  $\sigma_{22}$  at order zero divided by  $\lambda + 2\mu$  (Fig. 5(b)).

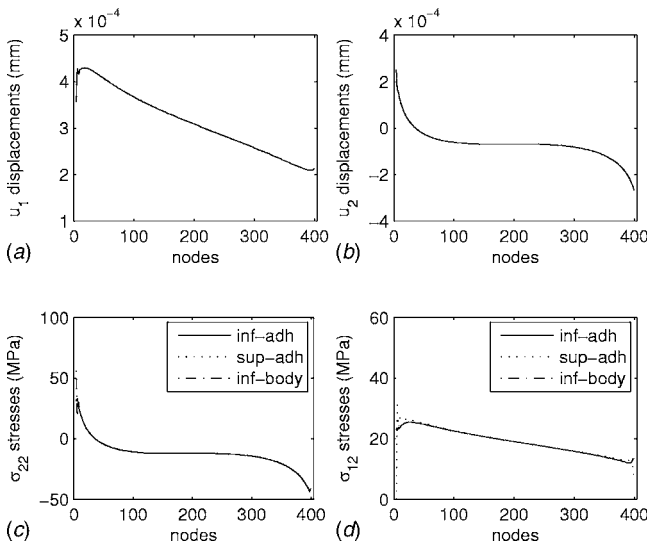


Fig. 4 Square bar: numerical results on the contact zone: (a)  $u_1$  displacements; (b)  $u_2$  displacements; (c)  $\sigma_{22}$  stresses; (d)  $\sigma_{12}$  stresses (-) lower zone on the adhesive, (...) upper zone on the adhesive, (-) lower zone on the elastic body

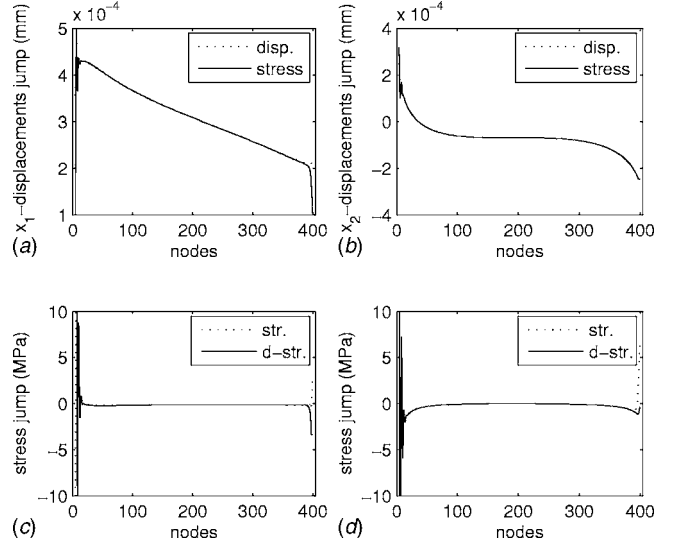


Fig. 5 Square bar: numerical results on the contact zone: (a)  $[u_1]$  displacements; (b)  $[u_2]$  displacements; (c)  $[\sigma_{12}]$  stresses; (d)  $[\sigma_{22}]$  stresses (... jump in the stress, (-) derivative)

3.1.2.4 *Jump in the stress vector at order 1 (Eqs. (8c) and (8d)).* At order one, it can be seen from Fig. 4 that the stresses are very small. This is computed by dividing the numerical displacement obtained in the upper nodes of the layer by  $\varepsilon$ . Stresses at order zero are computed in the upper nodes of the layers. For Eqs. (8c) and (8d), the jump in the stress vector at order one is taken to be equal to the difference between the values obtained in the upper and lower nodes of the layer. Figure 5(c) shows that stress  $\sigma_{12}$  (denoted str.) is similar to the derivative of  $\sigma_{22}$  (denoted d-str.) at order zero (upper nodes of the layer) divided by  $\lambda/(\lambda + 2\mu)$ . The derivatives of the stresses at order zero are computed in the upper nodes of the layer. In Fig. 5(d), we can see that the jump in the stress  $\sigma_{22}$  at order one is approximately zero as predicted in Eq. (8c).

3.1.2.5 *Conclusion.* In Fig. 5, we have checked the results by comparing each term of Eqs. (8). The agreement found to exist between the curves confirms the validity of the theory presented in Ref. [2] and developed in this paper. One notes a divergence of the theory on the edges. From a mathematical point of view, this theory is valid only in the open set and not in the closed set. This problem will be taken into account thereafter.

## 3.2 Second Numerical Example

3.2.1 *Geometry of the Problem.* In this section, we describe numerical tests performed on two bars connected with a thin layer (Fig. 6). The width of the bars is equal to 99.5 mm and the thickness of the thin layer is equal to 1 mm. The lower bar is clamped underneath. A horizontal load is applied to the whole left side of the top bar and a vertical one is applied to the upper left part of the top bar.

### 3.2.2 Numerical Synthesis

3.2.2.1 *Jump in the displacements at order 0 (Eqs. (7a) and (7b)).* The first step in the numerical validation procedure consists of checking that the values of the jump in the displacements at order zero tend toward zero. In this example, the jump in the displacements is equal to the difference between the displacements of the upper nodes and the lower nodes of the thin layer. The jump was found to be small (Figs. 7(a) and 7(b)). The values of the jumps tend to zero. These values are in the  $[2 \cdot 10^{-4}, 5 \cdot 10^{-4}]$  mm range with  $u_1$  and in the  $[-2 \cdot 10^{-4}, 1 \cdot 10^{-4}]$  mm range with  $u_2$ .

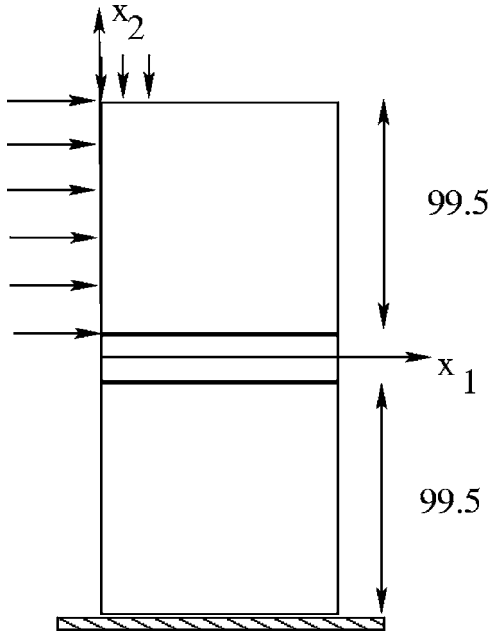


Fig. 6 Second example: two bonded bars (dimensions in mm)

3.2.2.2 *Jump in the stress vector at order 0* (Eqs. (7c) and (7d)). In the case of the stress vector, we computed the stress difference between the lower and upper nodes of the layer (Figs. 7(c) and 7(d)). The two values were found to be similar and the jump tends toward zero.

3.2.2.3 *Jump in the displacements at order 1* (Eqs. (8a) and (8b)). In this case, the thin layer is not bonded directly with a rigid body and the terms in Eqs. (8a) and (8b) are not simplified. The jump in the displacements at order one is taken to be the computed jump in the displacements divided by  $\varepsilon$ . The derivative of the displacement (Eqs. (8a) and (8b)) is approximated for the upper nodes of the thin layer. We compared Eqs. (8a) and (8b) with the numerical jump in the displacement at order one (denoted disp. in Fig. 8). It can be seen from Figs. 8(a) and 8(b) that these values are very similar.

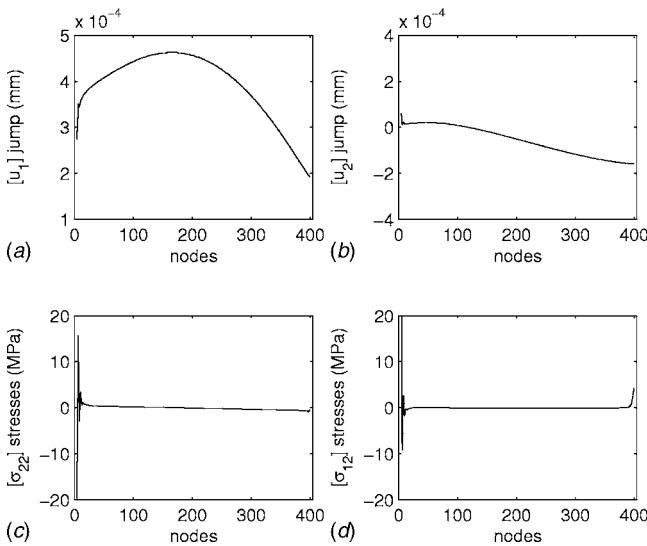


Fig. 7 Two bars: numerical results on the contact zone: (a)  $[u_1]$  displacements; (b)  $[u_2]$  displacements; (c)  $[\sigma_{22}]$  stresses; and (d)  $[\sigma_{12}]$  stresses

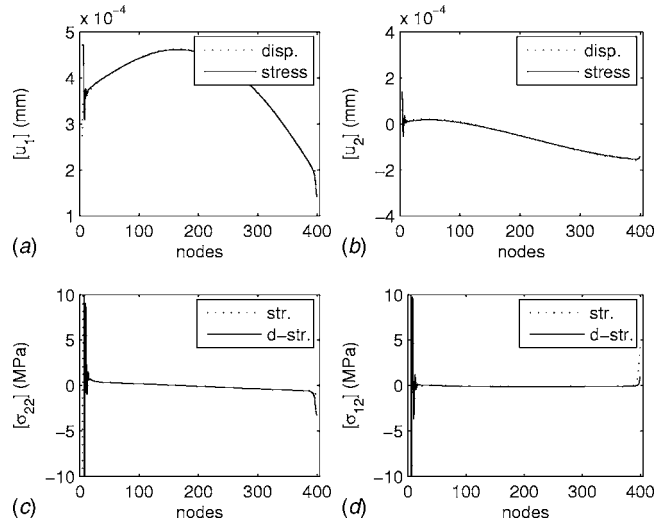


Fig. 8 Two bars: numerical data on the contact zone (a)  $[u_1]$  displacements; (b)  $[u_2]$  displacements (... displacements, - stress); (c)  $[\sigma_{22}]$  stresses; (d)  $[\sigma_{12}]$  stresses (... jump in the stress, (-) derivative)

3.2.2.4 *Jump in the stress vector at order 1* (Eqs. (8c) and (8d)). In Eqs. (8c) and (8d), the jump in the stress vector at order one is taken to be equal to the difference between the values in the upper and lower nodes of the layer. The derivatives of the stresses at order zero are computed in the upper nodes of the layer. As Fig. 8(c) shows, stress  $\sigma_{12}$  (denoted str.) is similar to the derivative of  $\sigma_{22}$  (denoted d-str.) at order zero (upper nodes of the layer) divided by  $\lambda/(\lambda+2\mu)$  (Eq. (8d)). In Fig. 8(d), we can see that the jump in stress  $\sigma_{22}$  at order one is similar to the values obtained upon computing the right hand side of Eq. (8c).

3.2.2.5 *Conclusion.* The numerical data given in Fig. 8 are compared with the theoretical results obtained in each term of Eq. (8). The good agreement obtained confirms the validity of the theory proposed in Ref. [2].

#### 4 Comments on Concentrated Forces at the Edges

As seen in the previous sections (Figs. 4, 5, 7, and 8), the results presented in Eq. (8) are no longer valid near the edges. In this case, it is necessary to include concentrated forces in the model. In particular, the limit model does not take into account the singularities of stresses on the edges. In this paragraph, one presents a way of taking into account partial effects of the singularities near the edges. Let us consider a small circle centered at the edge of the thin layer (see Fig. 9). Using the divergence formula and Eqs. (1), (4), and (6) (i)(vii), we obtain

$$\int_{C_\varepsilon} \sigma n + \int_{D_\varepsilon} \sigma n = 0$$

$$\int_{C_\varepsilon} \sigma^1 n + \int_{-1/2}^{-1/2} \tau^0 n = 0$$

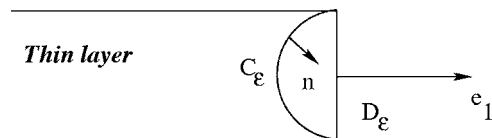
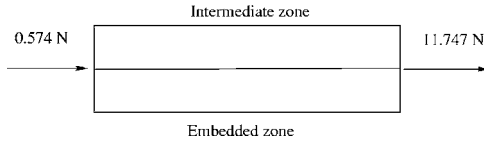


Fig. 9 Concentrated forces



**Fig. 10 Application of the concentrated forces**

$$\int_{C_e} \sigma^1 n = - \left( \frac{4\mu(\lambda + \mu)}{\lambda + 2\mu} \frac{\partial u_1^0}{\partial x_1} - \frac{\lambda}{\lambda + 2\mu} \sigma_{22}^0 \right) e_1 \quad (9)$$

Therefore the concentrated forces at the edges  $P^\pm$ , denoted  $F$ , are

$$F = - \left( \frac{4\mu(\lambda + \mu)}{\lambda + 2\mu} \frac{\partial u_1^0}{\partial x_1} - \frac{\lambda}{\lambda + 2\mu} \sigma_{22}^0 \right) (P^\pm) e_1 \quad (10)$$

The validity of these theoretical results can be seen by comparing Eq. (10) with the computed numerical data. We applied to the limit problem (first example) a concentrated force exerted on the first line of elements as shown in Eq. (10). The value of this force is obtained by performing computations on the real data (see Fig. 10). In Fig. 11, the limit problem with and without concentrated forces and the initial problem with the thin layer are compared. The results show the considerable improvement obtained in the case involving concentrated forces (Fig. 11).

## 5 Conclusion

In this study, we have both developed and numerically validated an asymptotic model for the interface described in Ref. [2]. This interface model is nonlocal. Good agreement was obtained between theoretical and numerical data. One obtains a law that could be modeled numerically at order 1 by particular cohesive elements. We now intend to develop a theory on similar lines dealing with the nonlinear constitutive laws pertaining to the thin layer, in particular, taking into account damage or heterogeneities (as in adhesives reinforced by particles).

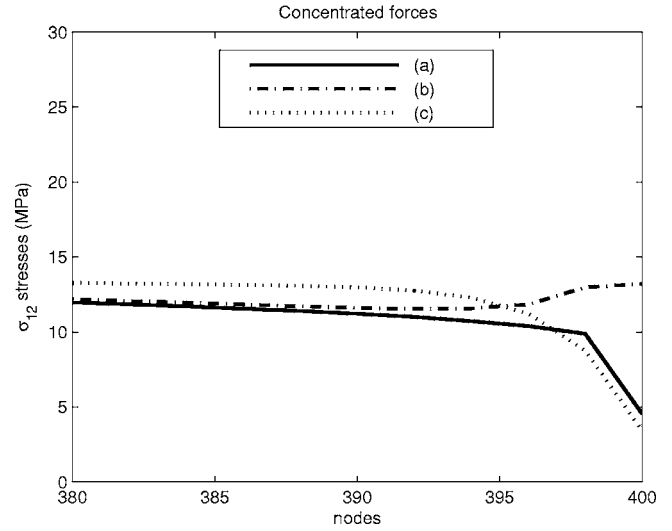


**Fig. 11 Numerical solution on the edge (a) limit problem with concentrated forces; (b) limit problem without concentrated forces; and (c) initial problem with two layers**

## References

- [1] Lebon, F., and Ronel-Idrissi, S., 2004, "Asymptotic Analysis of Mohr-Coulomb and Drucker-Prager Soft Thin Layers," *Steel Compos. Struct.*, **4**, pp. 133–147.
- [2] Abdelmoula, R., Coutris, M., and Marigo, J. J., 1998, "Comportement Asymptotique d'une Interface Élastique Mince," *C. R. Acad. Sci. III*, **326**, pp. 237–242.
- [3] Sanchez-Palencia, E., 1980, "Non Homogeneous Materials and Vibration Theory," *Lecture Notes in Physics*, Springer, Berlin, Vol. No. 127.
- [4] Eckhaus, W., 1979, *Asymptotic Analysis of Singular Perturbations*, North-Holland, Dordredht, The Netherlands.
- [5] ANSYS, 2002, ANSYS 6.1, SASIP.